L-vehicles Emissions and Noise mitigation Solutions

D3.2 Method and system for on-board noise measurement

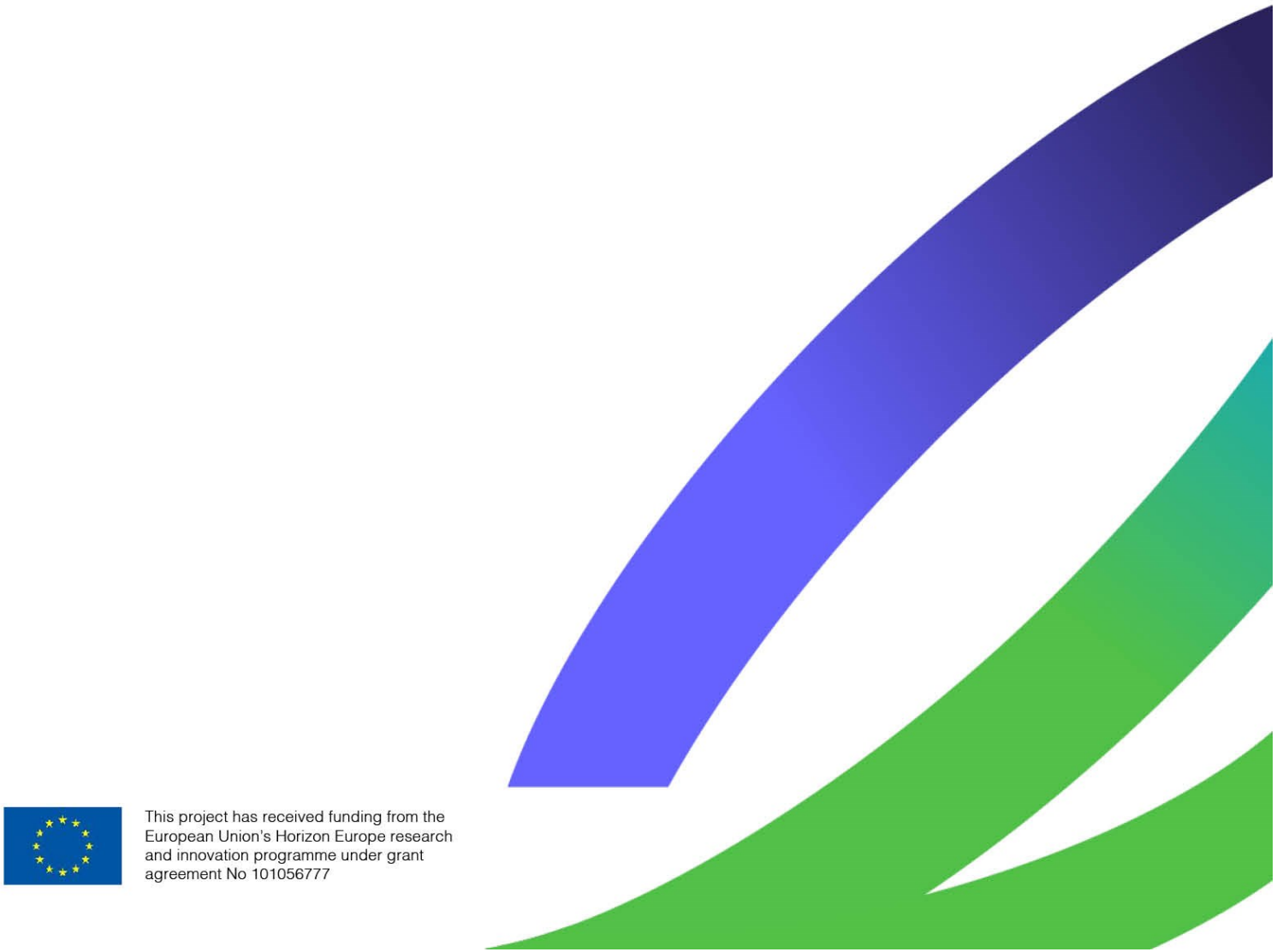

This project has received funding from the European Union's Horizon Europe research and innovation programme under grant agreement No 101056777

Deliverable No.	D3.2	
Deliverable title	Method and system for on-board noise measurement	
Deliverable type	DEM – Prototype	
Dissemination level	Public	
Deliverable leader	RWTH Aachen (ika)	
Contractual due date	31.08.2023	
Actual submission date	20.11.2023	
Version	1.0	
Written by	Carina Diemel, Olaf Uszynski (RWTH Aachen (ika))	10.10.2023
Reviewed by	Åke Sjödin (IVL)	17.10.2023
	Silvia Fodera' (PIAGGIO)	20.10.2023
Approved by	All partners	17.11.2023

Revisions table

Version	Date	Change
1.0	20.11.2023	First submission to the EC

This project has received funding from the European Union's Horizon Europe research and innovation programme under grant agreement No 101056777

Table of contents

This project has received funding from the European Union's Horizon Europe research and innovation programme under grant agreement No 101056777

Executive summary

This deliverable is part of the LENS project and focuses on the development process of an on-board sensor system for monitoring noise and location data of L-category vehicles. It is well known, that these vehicles cause high noise emissions especially during highly dynamic driving scenarios. Therefore, the type approval regulations for L-category vehicles were revised in the past. This arises the question, if the driving scenarios specified in the type approval tests cover real-world driving conditions of L-category vehicles. Therefore, the on-board system will be used under real driving patterns to capture noise in parallel with location data. Key components of the sensor system are the microphone and the GPS module. The development process goes through various stages, from component selection to software implementation and mechanical housing design. The system is verified in comparison to a microphone of a high accuracy class (class 1) in a semi-anechoic chamber. Further, on-board noise measurements are conducted with four class 1 microphones at various positions in order to define a suitable mounting position. This deliverable is a contribution for the planned measurement campaign in order to identify driving situations that cause high noise emissions as part of the post-processing and later to derive a realistic driving cycle.

This project has received funding from the European Union's Horizon Europe research and innovation programme under grant agreement No 101056777

List of abbreviations

BN	Background noise
C	Constant driving
CAD	Computer Aided Design
CO	Coasting
CPU	Central processing unit
ECM	Electret condenser microphone
FA	Full-load acceleration
G	Gears
GPIO	General Purpose Input/Output
IoT	Internet of Things
I2C	Inter-Integrated Circuit
I2S	Inter-IC Sound
LED	Light Emitting Diode
MEMS	Micro-Electro-Mechanical-Systems
PA	Partial load acceleration
RDE	Real Driving Emissions
RTOS	Real-Time Operating System
SF	Stationary full rpm
SP	Stationary partial rpm
SPI	Serial Peripheral Interface
SPL	Sound Pressure Level
SRAM	Static random-access memory
T	Test cycles
UART	Universal Asynchronous Receiver / Transmitter

This project has received funding from the European Union's Horizon Europe research and innovation programme under grant agreement No 101056777

List of figures

List of tables

This project has received funding from the European Union's Horizon Europe research and innovation programme under grant agreement No 101056777

1 Introduction

1.1 Background and objectives

High noise levels as well as pollutant emissions are harmful factors to human health and the environment. L-category vehicles like mopeds or motorcycles can cause significant noise and pollutant emissions. The type approval regulations mainly consider standard driving conditions, which mostly do not cover driving scenarios that lead to particularly high sound pressure levels and pollutant emissions. Therefore, the noise and pollutant emissions behaviour of L-category vehicles has to be investigated under real-world driving conditions. In order to analyse real driving patterns the L-vehicles Emissions and Noise mitigation Solutions (LENS) project aims among other topics to develop and apply techniques for monitoring noise and exhaust emissions.

This report is part of Work Package WP3, that covers the On-road RDE measurements of noise and exhaust emissions within the LENS project. Particularly, this report covers Deliverable D3.2, which addresses the development of a Method and system for on-board noise measurement. As part of an on-road measurement campaign, a number of 14 different L-category vehicles will be equipped with the on-board sensor system. The collected data will be evaluated in order to identify driving conditions that lead to high noise levels. The following objectives are of particular importance for the development of the on-board sensor system:

- Literature review of existing on-board systems for logging noise and GPS data of L-category vehicles.
- Identification of suitable components for the sensor system.
- Software development for data logging.
- Mechanical housing design for easy handling, variable mounting on the vehicles and resistant to the expected environmental conditions.
- Identification of suitable mounting position on a vehicle.

Ten on-board systems will be manufactured and distributed among the project partners to enable measurements to be performed at various locations in the EU. The recorded data of the on-board systems will be utilized for the development of a realistic driving cycle that constitutes another deliverable of the LENS project.

1.2 Structure

This report is structured as follows: Chapter 2 deals with the overall design of the sensor system. This includes the component selection and software implementation as well as the housing design. Chapter 3 covers the verification process of the developed sensor system. Chapter 4 describes suitable mounting positions of the sensor system on the vehicle in more detail. The results of on-board noise measurements are presented and discussed in order to find a suitable mounting position for the sensor system. Chapter 5 provides a conclusion of the whole development process.

This project has received funding from the European Union's Horizon Europe research and innovation programme under grant agreement No 101056777

2 Sensor system design

This chapter outlines the development process of the on-board system. In order to develop a suitable sensor system for the on-board application on L-category vehicles, a literatur review regarding existing data logging systems is conducted.

2.1 Literature review

The focus lies on literature regarding sensor systems for noise recording and GPS data logging. Particularly, most of the examined literatures do not address a simultaneous monitoring process of noise and GPS data, but provided an initial starting point for the development process of the LENS sensor system. Gunatilaka [1] developed an acoustic sensor device with a microcontroller and a digital microphone to capture environmental noise. The audio data is transmitted to a cloud server using IoT technology. Picaut et al. [2] provide a comprehensive overview of literatures that focus on IoT technology for monitoring noise data and set a special focus on the microphone selection. The latter is also of major importance for the development process of the LENS sensor system, since the advantages of a special microphone type are presented. Peeters and v. Blokland [3] address the on-board monitoring of noise emissions of L-category vehicles. Three L-category vehicles where equipped with the data logging system that captures the noise of the engine intake and exhaust, the vehicle and engine speed as well as the throttle position. However, due to its dimensions and the way of mounting, the system may not be suitable for all L-category vehicles. The introduced literature provided a general overview of the existing sensor systems.

2.2 Selection of components

The first step in the course of component selection is to establish the requirements in the context of the use case. For this purpose, the main functionalities of the sensor system were defined. A continuous monitoring of audio data and GPS positioning data under real-world driving conditions is a major task of the sensor system. The monitored audio data should have a high dynamic and frequency range. The GPS module provides positioning data for localisation and derivation of the altitude as well as frequently driven routes and allows a correlation between location and critical driving scenarios (e.g., intersection / traffic light). Additionally, the GPS data enable the derivation of speed, as this cannot be determined from the vehicle due to vehicle-specific restrictions (e.g., OBD connector). The captured data is stored without transmission to a server. The reason for this is that the server connectivity must be ensured, otherwise data loss will occur. Therefore, the data is stored locally on a microSD card in the sensor system. In addition, the dimensions of the system should be small in order to ensure easy and fast mounting on different vehicles. Further, the components should be cost-effective due to the high number of devices (10) to be build. Other requirements are that the user interfaces should be easy to use and the housing should protect the components from environmental influences. In general, the system should work autonomously in order to attach it to a wide variety of L-category vehicles. According to these requirements, the components were selected.

This project has received funding from the European Union's Horizon Europe research and innovation programme under grant agreement No 101056777

First, research was conducted on the components available on the market and suitable for the use case. The core of the system is a central data processing unit to control the peripherals. Various single board computers and microcontrollers are conceivable for this application. Due to the on-board operation, a battery will power the system. Therefore, a board is selected due to its low-power consumption, its integrated battery port, its small dimensions, its processing performance and its suitable communication protocols.

The FireBeetle ESP32 IoT Microcontroller from DFRobot meets the above-mentioned requirements. Figure 2-1 shows the ESP32 together with its pinout. The microcontroller has an operating voltage of 3.3 V and a CPU Frequency of 240 MHz [4]. The size of the SRAM is 520 kB and the flash memory size is 16 MB [4]. The ESP32 is equipped with a Dual-Core-ESP-WROOM-32 module and supports dual-mode communication as well as further capabilities such as Wi-Fi and Bluetooth [4].

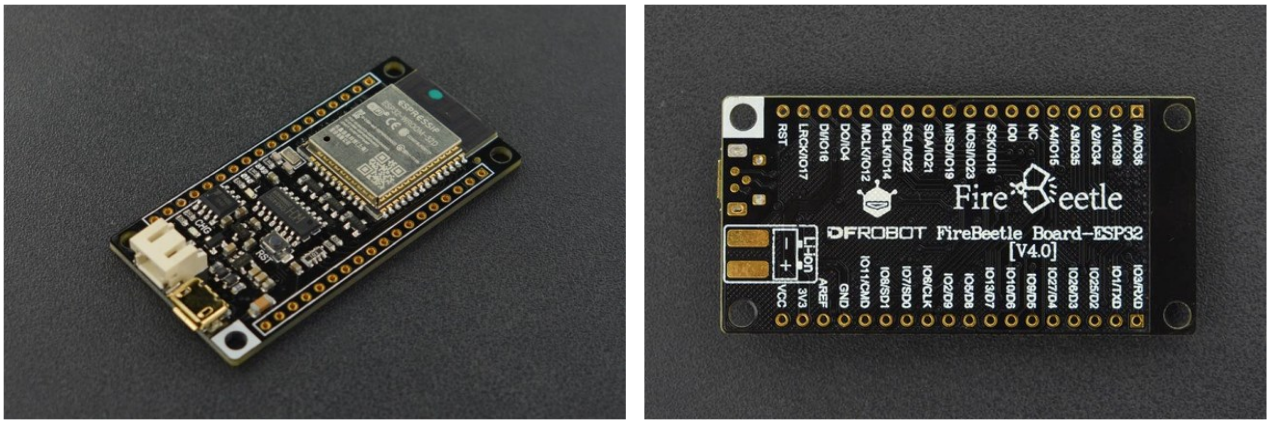

Figure 2-1: FireBeetle ESP32 IoT Microcontroller [4]

The Dual-Core system enables tasks running on different cores using FreeRTOS [9]. In addition, the microcontroller supports the following communication protocols: UART, I2C, I2S, SPI, etc. [4]. These protocols are relevant for the communication with the peripherals, i.e., the GPS module and the microphone. The pinout defines the usage and the communication protocol type for the GPIO pins. The microcontroller is compatible with MicroPython, the Arduino IDE and further programming environments/languages [4].

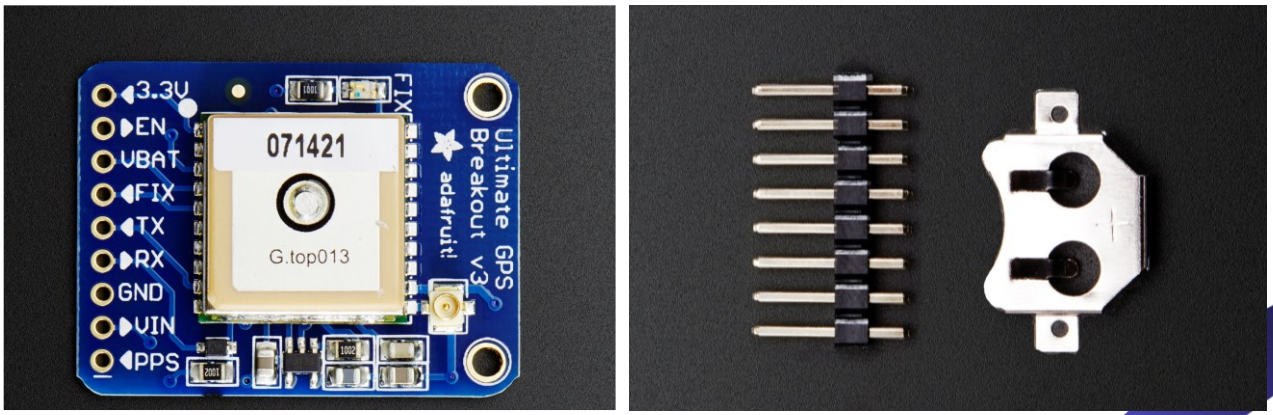

Figure 2-2: Adafruit Ultimate GPS Module [5]

This project has received funding from the European Union's Horizon Europe research and innovation programme under grant agreement No 101056777

In order to monitor the GPS data and thus, derive the vehicle speed, the Adafruit Ultimate GPS module is selected, which is capable of tracking up to 22 satellites on 66 channels [5]. Furthermore, the GPS module has an update rate of 1 to 10 Hz, a position accuracy of 1.8 meters and a velocity accuracy of 0.1 meters/s [5]. Figure 2-2 shows the GPS module from the front side together with a battery holder. The CR1220 battery holder is placed on the backside of the GPS module. If the GPS module does not have a fix, the LED is blinking at approximately 1 Hz as visual feedback for the user [5]. After the GPS module has found satellites, the LED is blinking once every 15 seconds [5].

The literature review by Picaut et al. [2] stated that three microphone types are commonly used for sensor systems. These include the electret condenser microphones (ECM) and the analog or digital MEMS microphones. The MEMS microphones were preferred compared to the ECMs due to their acoustic performance. Further advantages mentioned in [2] include e.g., reliability, smaller dimensions and lower production costs. Therefore, the preferred choice for the LENS sensor system is a digital MEMS microphone that allows I2S communication. The Adafruit I2S MEMS microphone is selected for the sensor system [6]. The MEMS microphone covers a frequency range from 50 Hz to 15 kHz [7]. The front and backside of the MEMS microphone breakout board is illustrated in Figure 2-3. The Knowles SPH0645LM4H-B microphone is mounted on the breakout board, which can be wired to the I2S interface of the ESP32. The acoustic overload point of the microphone is 120 dB(SPL) [7].

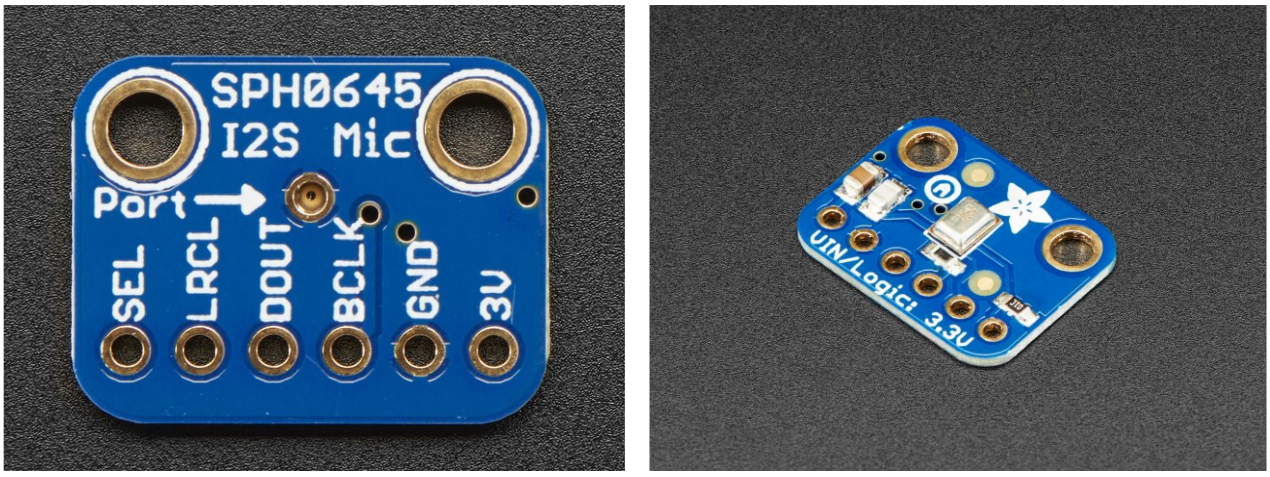

Figure 2-3: Adafruit I2S MEMS microphone breakout board [6]

The GPS and microphone data are stored on a microSD card. For this purpose, a microSD card breakout board is required. For the on-board system, the breakout board from Adafruit is selected [8]. Figure 2-4 provides a picture of the front side of the breakout board. The microSD card can be easily removed from the breakout board. The breakout board can be wired up to the SPI interface of the microcontroller [8]. MicroSDHC cards of different sizes (e.g., 4 GB or 8 GB) can be mounted and enable suitable data storage.

This project has received funding from the European Union's Horizon Europe research and innovation programme under grant agreement No 101056777

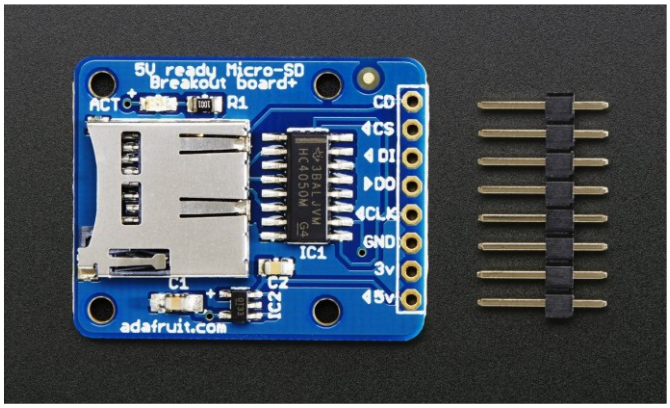

Figure 2-4: Micro SD Card Breakout Board [8]

A LiPo battery with an electrical charge of 2500 mAh powers the sensor system. With an average working current of 80 mA of the ESP32 [4] an average operating time of about 30 hours should be possible. Further components provide interfaces to the user, such as a switch to start or stop the measurement process or LEDs as feedback for the user.

2.3 Circuit diagram and embedded software overview

The components are wired according to the pinout of the ESP32. Each component communicates via their corresponding interface with the ESP32. Figure 2-5 illustrates the wiring of the components to the GPIO pins of the microcontroller. All components are connected to the GND and 3.3 V pin of the ESP32. For a better overview, this has not been included in the figure.

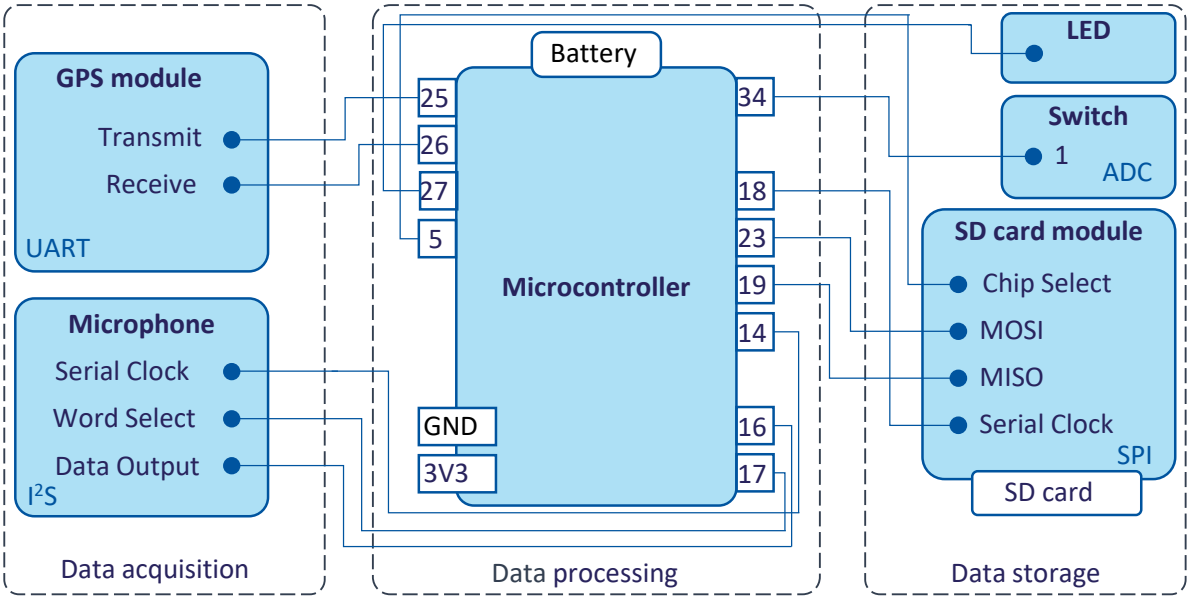

Figure 2-5: Wiring diagram of sensor system [16]

The microphone requires an I2S interface and therefore is connected to the GPIO pins 14, 16 and 17 of the microcontroller. The GPS module communicates via UART interface and is wired to the GPIO pins 25 and

This project has received funding from the European Union's Horizon Europe research and innovation programme under grant agreement No 101056777

26 of the microcontroller. The ESP32 is a board with hardware serial support. The microSD card breakout board is connected to the SPI interface of the microcontroller; this includes the GPIO pins 5, 23, 19 and 18. The micropohone and the GPS module conduct the data acquisition. The ESP32 processes the data and stores them on the microSD card. The readout ADC value of the switch is a threshold for starting or stopping data logging. The software implementation is realized with the Arduino IDE, which supports the programming language C++. To use the dual-core mode of the ESP32, FreeRTOS, a real-time operating system for microcontrollers [9], is applied. The tasks for logging and storing data will be defined and exectuted on core 0 and 1. This allows efficient usage of both cores. After switching the device on, the LED turns on and the tasks for reading the incoming microphone and GPS data start. Both datasets are processed in the storage tasks. The GPS and microphone data are simultaneously read and alternately stored on the microSD card. When the measurement is finished, the user turns off the switch and the stored file is closed.

2.4 Mechanical Housing Design

To protect the components from environmental influences and to mount the system on the vehicles, a housing is designed. The main requirements are to enable simple and fast mounting on various L-category vehicles as well as the alignment of the GPS antenna and the MEMS microphone port. In addition, it is to be guaranteed that the components are fixed, to avoid the microphone to capture interfering rattling noise.

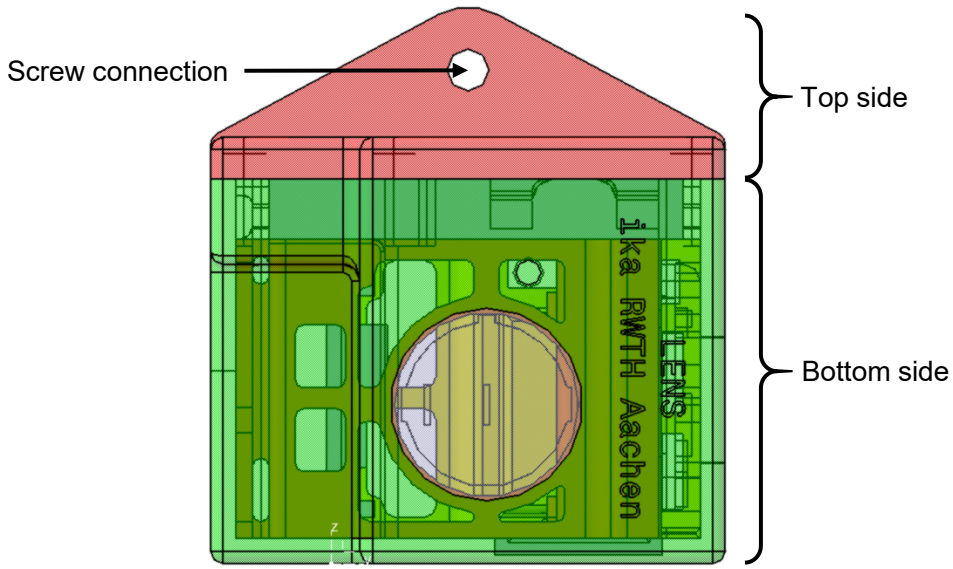

Figure 2-6: CAD model – Front side of the mechanical housing

Figure 2-6 shows the front side of the CAD model of the housing. The housing consists of a top and bottom side. The components are positioned inside the bottom side. The top side is equipped with a mechanism for attaching a screw connection. The isometric view of the CAD model is shown in Figure 2-7. The top side is screwed to the bottom side via M2 screws. The housing has a compact design and outer dimensions of 80 x 62 x 66 mm.

This project has received funding from the European Union's Horizon Europe research and innovation programme under grant agreement No 101056777

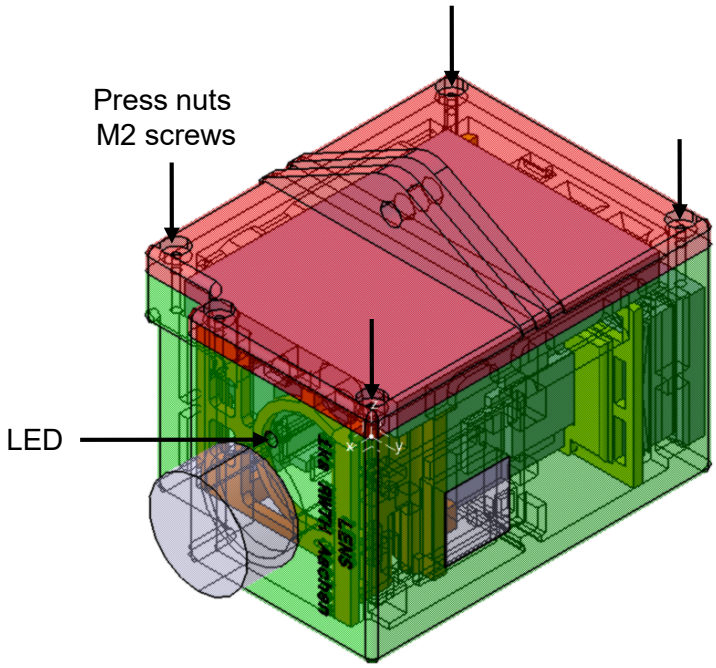

Figure 2-7: CAD model - Isometric view of the mechanical housing

Figure 2-8 illustrates two additional side views of the mechanical housing. A switch is placed in the wall of the housing, which is used to start or stop data logging. An opening for the GPS antenna is provided as shown in Figure 2-8. On the opposite side of the GPS module, the MEMS microphone is embedded in the housing. A small opening in the housing is provided for the port of the MEMS microphone. The microphone is protected from dust and splash water by an acoustic vent [10]. The acoustic vent is applied to the inner side of the housing. In addition, a slot is provided that allows easy removal of the microSD card. The screw connections do not have to be removed for this purpose.

The housing was additively manufactured. It is made of polyamide (PA12), which has a melting temperature of 172–180 °C and a high mechanical strength [11]. PA12 has a lower concentration of amides in comparison to other PA plastics and therefore absorbs less moisture and is more resistant to chemicals such as oil [15]. Figure 2-9 provides an overview of the different housing parts. The upper pictures of the figure show the front and back sides of the housing cover. The LiPo battery is inserted into the cover and will be plugged into the port of the ESP32. The pictures in the middle illustrate the inner framework of the housing, which is inserted into the bottom side of the housing. The SD card breakout board, the ESP32 and the MEMS microphone are attached to the framework. The inner framework holds the components firmly in their position. Circular and rectangular recesses are provided in the inner framework for the switch and the wires. The framework also stabilises the position of the battery. The SD card breakout board is connected via a recess in the inner framework to the housing opening for the SD card slot. The pictures below show the closed and open housing. The switch and the GPS antenna are inserted into the provided openings. The switch and LED provide interfaces to the user and simplifiy the operability of the system.

This project has received funding from the European Union's Horizon Europe research and innovation programme under grant agreement No 101056777

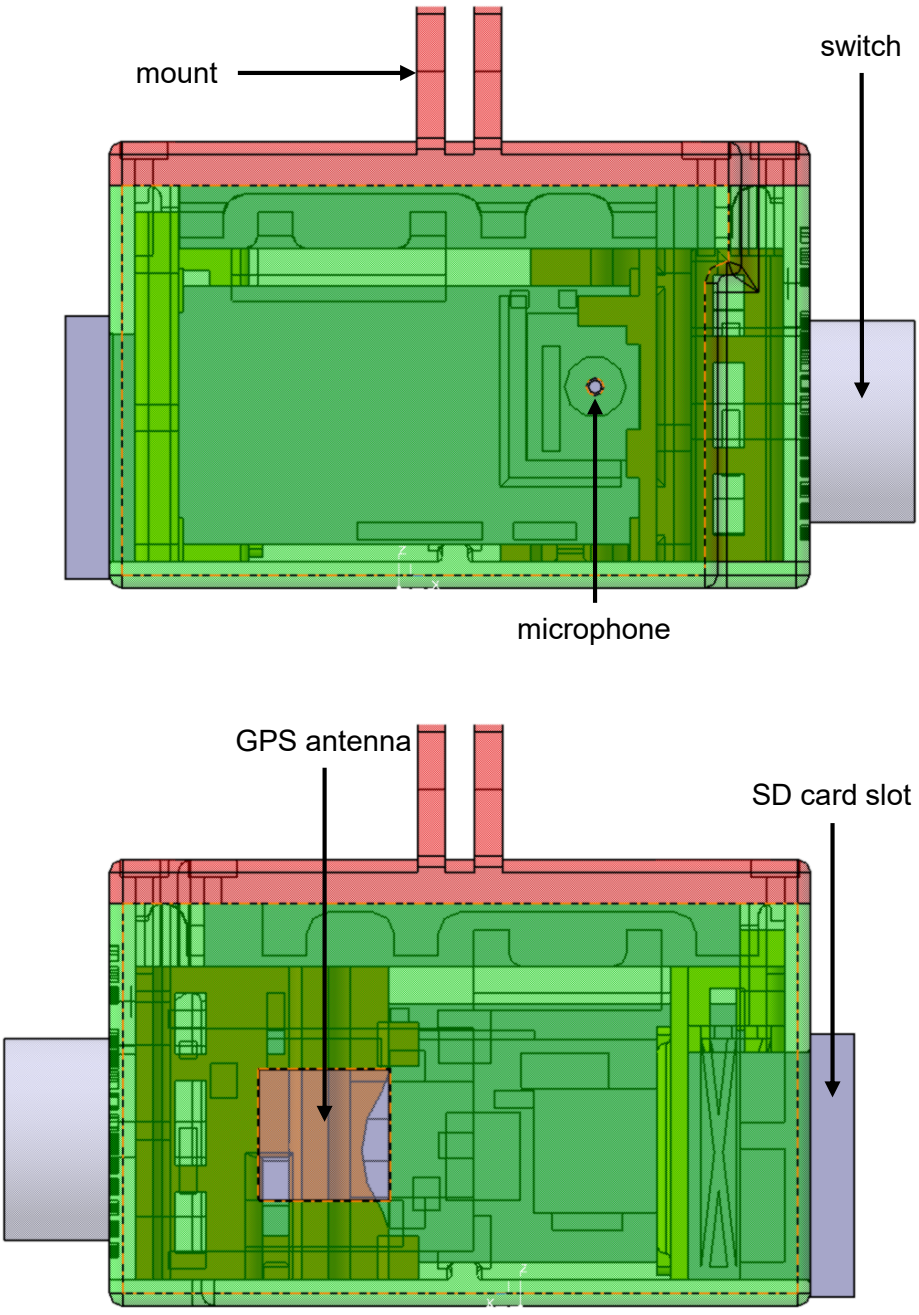

Figure 2-8: CAD model – Side views of the mechanical housing design

This project has received funding from the European Union's Horizon Europe research and innovation programme under grant agreement No 101056777

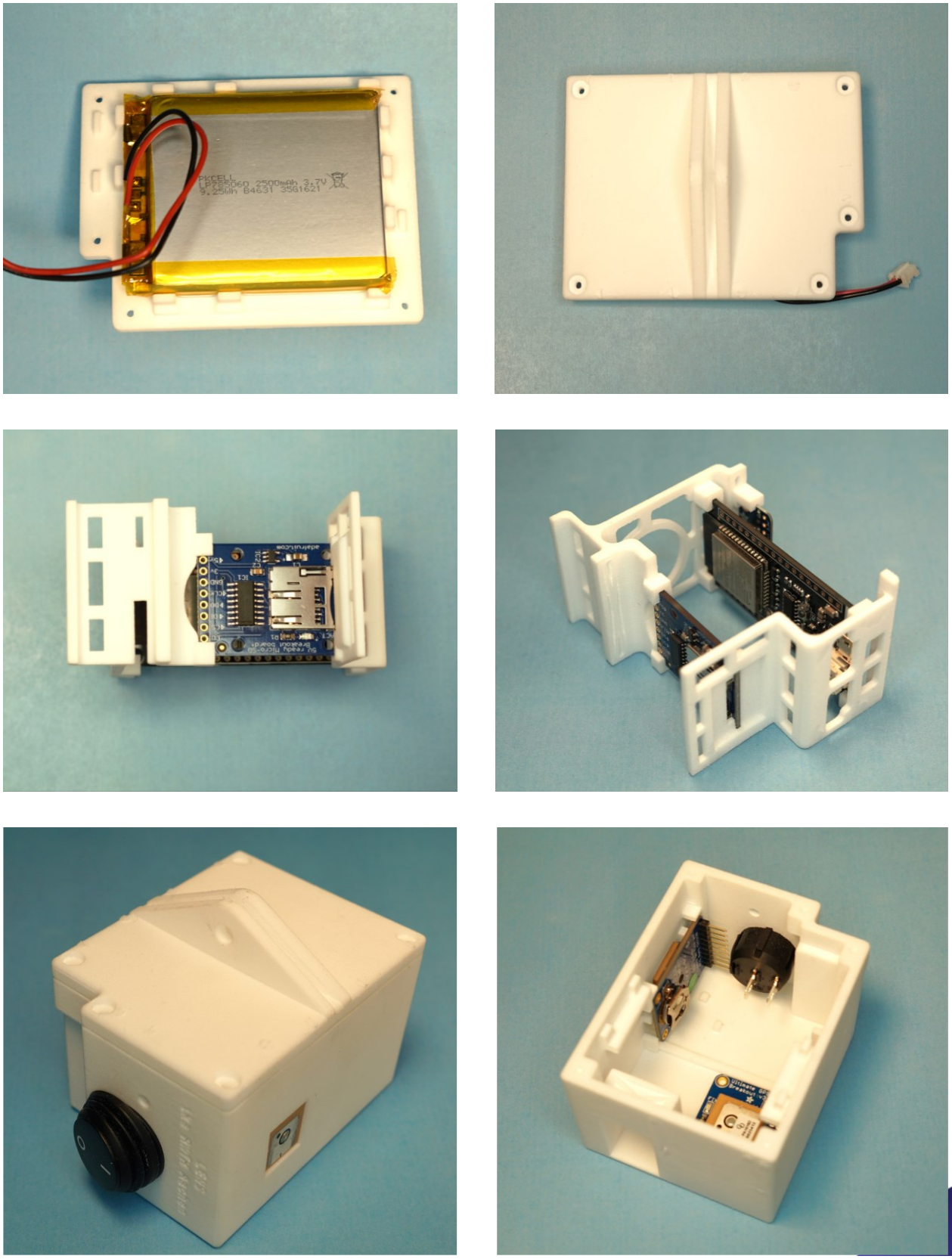

Figure 2-9: Top: Front / Back view of the cover; Middle: Internal framework; Bottom: Closed and open housing

This project has received funding from the European Union's Horizon Europe research and innovation programme under grant agreement No 101056777

3 Verification

The housing and the acoustic vent affect the transmission characteristics of the developed sensor system. To assess the significance of this influence, the system is tested in a semi-anechoic chamber with various measurement setups. A two-stage verification process is conducted.

3.1 First verification stage

The first stage includes an influence analysis of the housing and the acoustic vent. Therefore, the measurement setup illustrated in Figure 3-1 is used. This picture shows the setup for the second verification stage, since the reference microphone is inserted. However, this setup is the same for the first verification stage. The only difference is that in the first stage the sensor system is tested with acoustic vent and cover, without acoustic vent but with cover and without both, the acoustic vent and the cover [16].

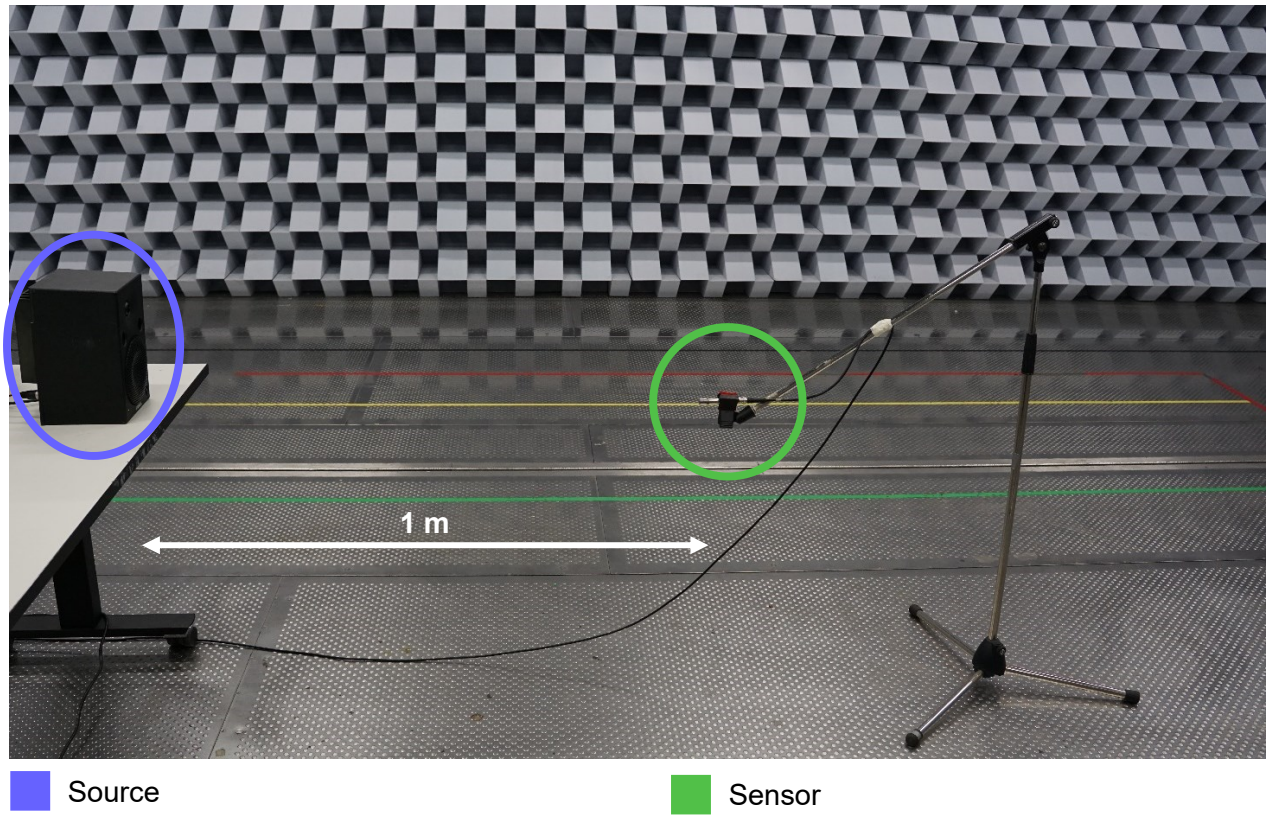

Figure 3-1: Measurement setup for the verification stages of the sensor system

A loudspeaker is placed at a distance of one meter to the sensor system, in this case the class 1 microphone. This microphone is replaced by the sensor system. The loudspeaker and the MEMS microphone of the sensor system are positioned at the same height. The loudspeaker generates a linear sine sweep from 100 Hz to 20 kHz with an increase of 331,67 Hz/s, resulting in a 60 s measurement duration. Furthermore,

This project has received funding from the European Union's Horizon Europe research and innovation programme under grant agreement No 101056777

a broadband white noise signal with a frequency range of 20 Hz to 20 kHz is considered. The loudspeaker position and the amplifier settings remain the same during all measurements [16].

As already mentioned, three different variations are tested this way. The testscenaries include measurements with and without cover or acoustic vent of the sensor system. The results of these measurements are evaluated by third-octave-spectra. Figure 3-2 shows the results for the sine sweep and the broadband noise signals [16].

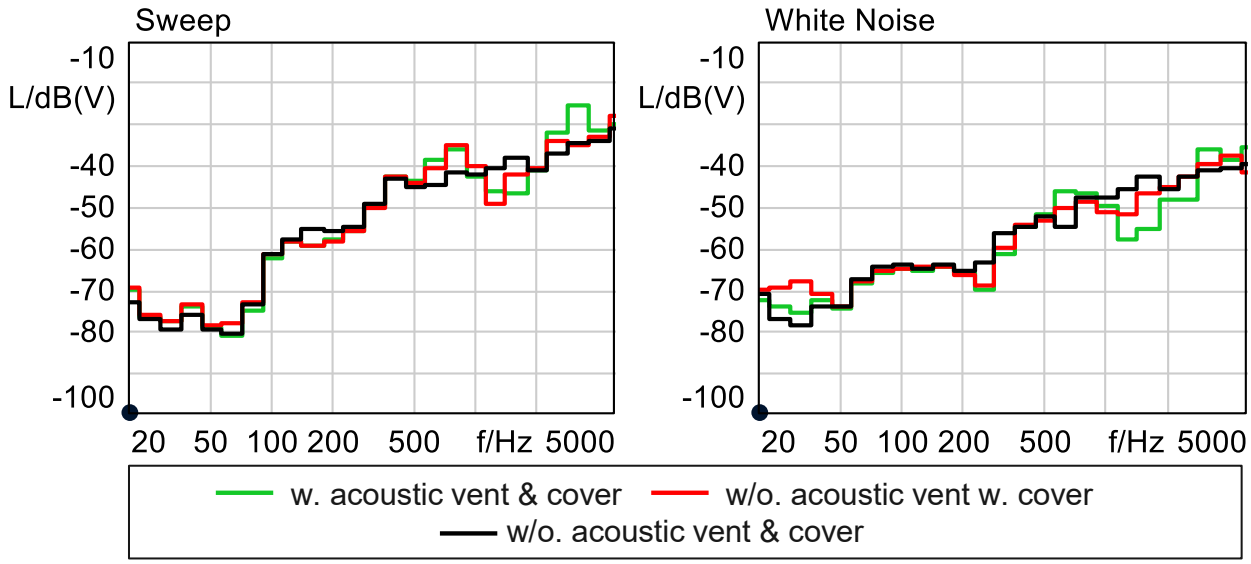

Figure 3-2: Influence of housing cover and acoustic vent on the transmission characteristic of the sensor in the third-octave spectrum [16]

The diagrams indicate that there are small differences between the three test scenarios in the range from 50 to 500 Hz. However, larger differences between the three test scenarios are noticeable above 500 Hz. The influence on the transmission properties of the cover and the acoustic vent can be reduced by applying signal processing methods, e.g., filtering, which are to be carried out during measurements on the vehicle in the later course of the project [16].

3.2 Second verification stage

Within the second stage of the verification process, the sound pressure sensitivity of the MEMS microphone is determined. Therefore, comparative measurements with a reference class 1 microphone are conducted. The previously mentioned measurement setup is kept for this verification stage. The comparison of the measured data provides the possibility to determine the sensitivity of the sensor system. Further, this enables the determination of the actual sound pressure level measured of the sensor system. Figure 3-3 shows a comparision of the reference microphone with the developed sensor system for both signals. The third-octave spectra of the reference microphone and the sensor system show similar results over a wide frequency range. The system shows an antiresonance at approximately 1000 Hz. Therefore, the frequency response should be corrected by suitable singal processing methods in the postprocessing. To conclude, the sensor system is suitable for enabling a qualitative comparison of driving patterns of various L-category vehicles [16].

This project has received funding from the European Union's Horizon Europe research and innovation programme under grant agreement No 101056777

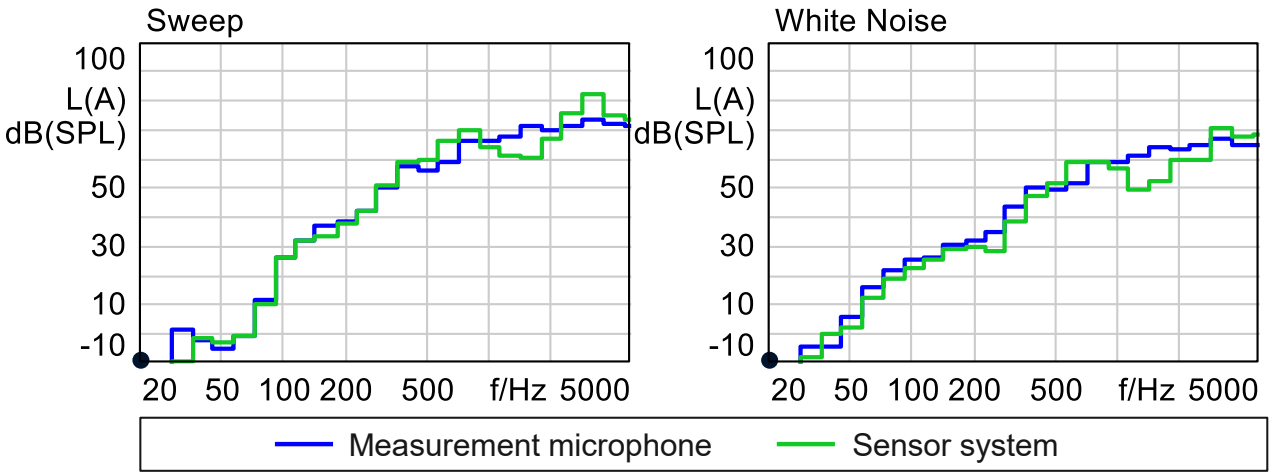

Figure 3-3: Comparison of one-third octave spectra of reference microphone and sensor system [16]

This project has received funding from the European Union's Horizon Europe research and innovation programme under grant agreement No 101056777

4 Positioning of the sensor system

In this section, a preliminary study based on measurements on test vehicles is described and analysed. The aim of these investigations is to determine the influence of the positioning of the sensor system on the vehicle in the context of the LENS project. Accordingly, it is not general differences in the measured sound pressure levels with varying microphone positions that are essential, but such differences that lead to the derivation of different critical driving maneuvers. Based on that, a suitable microphone position is derived.

4.1 Description of the measurement procedure

The measurements are to be performed on two exemplary vehicles. Due to their high proportion among L-category vehicles, a scooter-type motorcycle and a motorcycle are investigated. The relevant vehicle specifications are depicted in Table 4-1 for vehicle no.1 (V1) and vehicle no.2 (V2).

Table 4-1: Relevant specifications of the tested vehicles

Specification	V1	V2
Manufacturer	Yamaha	Honda
Model	SEH3 – YP125RA	JC84 - CBF125M
Type	Scooter-type motorcycle	Motorcycle
Category	L3e - A1	L3e - A1
Transmission	Continuously variable transmission	Mechanical transmission
Empty mass	167	117
No. of type approval	E13*168/2013*00985*03	E4*168/2013*00136*01
Displacement	125 cm³	124 cm³
Nominal power	9 kW	8 kW
Nominal rpm	8000	7500
Max. speed	99	95
Stationary noise	79 dB(A)	79 dB(A)
Driving noise	73 dB(A)	70 dB(A)

Both vehicles are equipped with four microphones of the highest accuracy class, class 1, i.e., PCB model HT378B02. With a frequency range of 3.5 to 20,000 Hz and a dynamic range of up to 138.5 dB, they cover the relevant audible range. These microphones are mounted with flexible arms and including windshields to minimize aeroacoustic noise disturbances, see. Figure 4-1. Three microphones are positioned in the

This project has received funding from the European Union's Horizon Europe research and innovation programme under grant agreement No 101056777

vehicle rear (left, middle and right) and one in the front. The lateral positioning of the microphones is intended to identify asymmetries in the directivity caused, for example, by the exhaust or the chain. Only strongly pronounced asymmetries are relevant, which can lead to critical driving scenarios not being detected. Also, in later investigations, i.e., in realistic operation, frequently run critical scenarios are to be identified. In addition, the positions of the microphones are chosen so that corresponding positions are available on most L-category vehicles in future studies. The position in the front of the vehicle is not to be considered in the further course of the project. It only serves as an extreme case with regard to positioning and the largest possible differences in levels are expected. It is to be examined in the first place whether critical driving scenarios are not detected with this position, since e.g., the vehicle could shield the noise of the exhaust. The test drives are carried out at the ika test track. The relevant information on dimensions and road surface properties can be found on the website [12].

Figure 4-1: Microphone setup (three in the back, one in the front) on the vehicles V1 (left) and V2 (right)

In order to determine the influence of microphone positions on the detection of critical driving maneuvers, different ones have to be defined. To represent realistic conditions, scenarios of full-load acceleration, part-load acceleration, background noise, constant driving at different speeds, stationary noise from idle up to maximum rpm as well as test cycles with a combination of the aforementioned are conducted. For

This project has received funding from the European Union's Horizon Europe research and innovation programme under grant agreement No 101056777

vehicle V2, some driving scenarios are tested several times in different gears. Here, the selection is made in such a way that all conceivable, relevant driving scenarios are covered.

4.2 Results of preliminary measurements

The first step is to identify the relevant frequency range. On the one hand, this examination is used for later settings of the measuring system, but also for post-processing. This is done on the basis of the full-load acceleration data, since these cover a wide frequency and speed range. Figure 4-2 (V1) and Figure 4-3 (V2) show the A-weighted sound pressure levels (SPLs) as a function of time and frequency. The sampling rate is 32768 Hz, the window length is 16384 Hz to ensure a time resolution of 0.5 s. Furthermore, a Hann window was used. In general, the typical course of the vehicle noise is well recognizable in both diagrams. On the one hand, there is the narrow-band, low-frequency noise, which only starts from 5 s, since it comes from the tire-road contact and is only present at higher speeds and on the other hand, but also primarily, the engine noise with its clearly recognizable harmonics. For both vehicles, the most dominant frequency range is up to 3 kHz. Above 5 kHz, the level almost drops to the background noise. For this reason, the important frequency range to be considered for future investigations is up to 5 kHz.

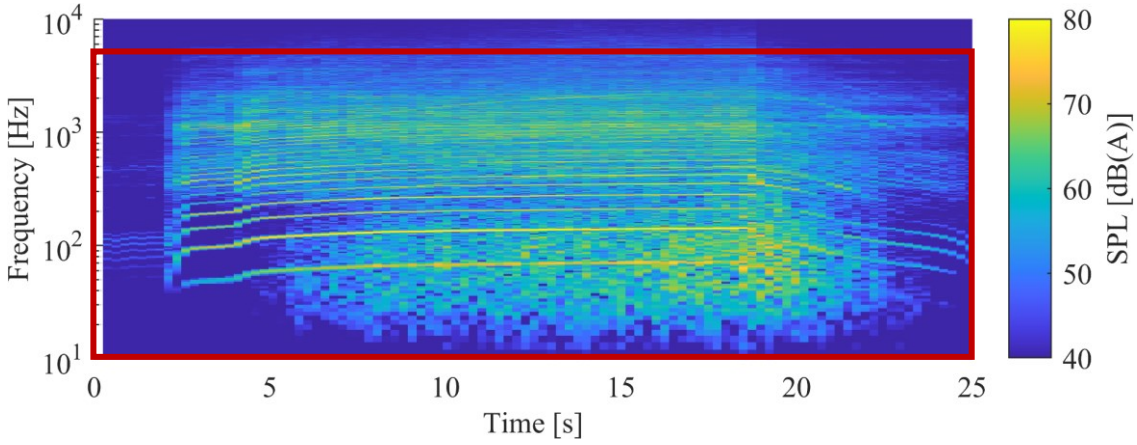

Figure 4-2: FFT vs. time for V1 full-load acceleration

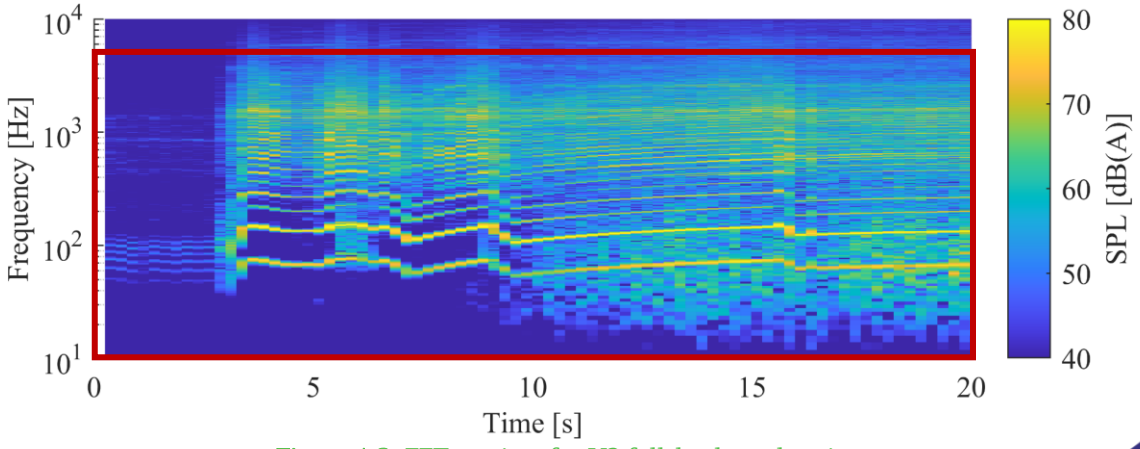

Figure 4-3: FFT vs. time for V2 full-load acceleration

This project has received funding from the European Union's Horizon Europe research and innovation programme under grant agreement No 101056777

Furthermore, the switching operations are very concise in Figure 4-3. In contrast, V1 shows a continuous increase without the pronounced gearshifts, which can be attributed to the continuously variable transmission. In a further step, the differences between the various microphone positions will be considered independently of the frequency distribution. For this purpose, Figure 4-4 and Figure 4-5 show the overall A-weighted sound pressure level over time. V1 had a final speed of approximately 85 km/h and the final speed of V2 was approximately 60 km/h. Here, all microphones show very similar patterns with only marginal differences. Furthermore, the microphones in the rear of the vehicle show almost the same level values with a mean standard deviation in the acceleration area of only $\sigma_{V1} = 0.67$ dB(A) for V1 and $\sigma_{V2} = 0.89$ dB(A) for V2. These results indicate that the position variation in the rear area is negligible for the vehicles considered.

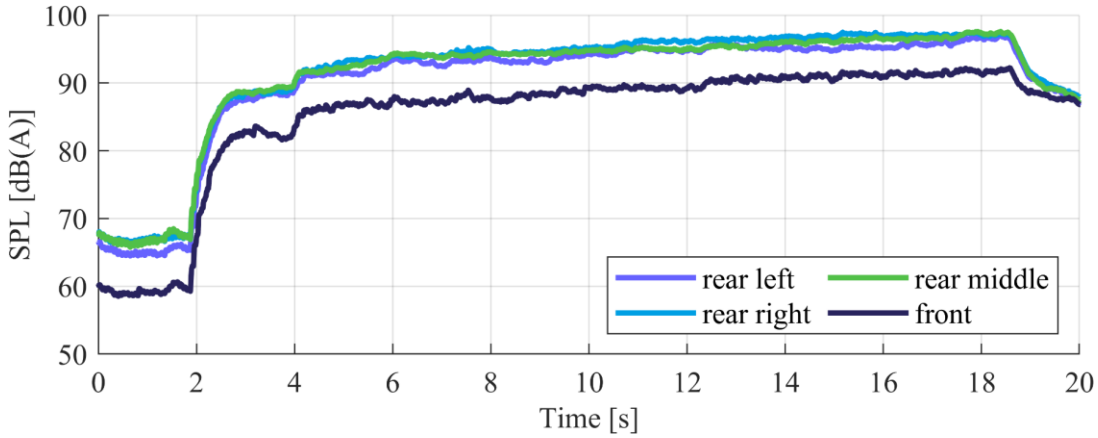

Figure 4-4: SPL vs. time for four microphone positions V1 full-load acceleration

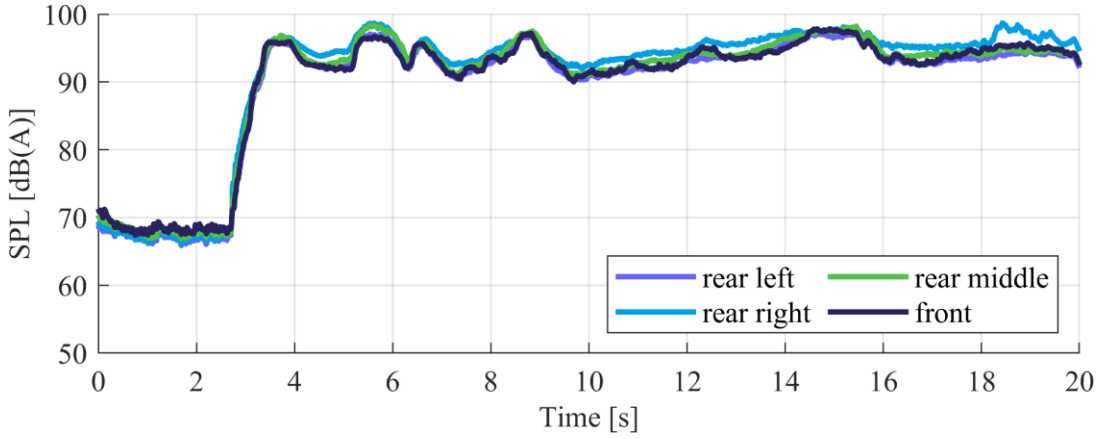

Figure 4-5: SPL vs. time for four microphone positions V2 full-load acceleration

However, when looking at the SPL, it can already be deduced that the values on the right microphone tend to be slightly higher. This can be attributed to the asymmetry of the vehicles, as the exhaust is on that side. At this point, the objective in the scope of the project is important and should be emphasized: Offsets are acceptable as long as they are constant to a good approximation for the relevant driving scenarios. In this regard, the results of the microphones in the front of the vehicles are of interest. V1 shows an almost constant high offset at the front position of $\Delta L_{V1} = -5.7$ dB(A), V2 only $\Delta L_{V2} = -0.7$ dB(A), which is due

This project has received funding from the European Union's Horizon Europe research and innovation programme under grant agreement No 101056777

to the different vehicle types/designs, i.e., location of critical sources such as the intake, and differently shielded front microphones. Nonetheless, these offsets are nearly constant, and the curves show the same pattern, so based on this data the same driving scenarios with all four microphones would be identified as relevant.

Furthermore, the corresponding plots for the constant speed of 30 km/h are shown, V1 in Figure 4-6 and V2 in Figure 4-7. Since this operating condition remains unchanged over time, no significant critical driving conditions can be determined. However, it can be clearly seen that the deviations of the microphones remain similar ($\sigma_{V1} = 0.75\ \mathrm{dB(A)}$ and $\sigma_{V2} = 1.00\ \mathrm{dB(A)}$; $\Delta L_{V1} = -6.00\ \mathrm{dB(A)}$ and $\Delta L_{V2} = -1.40\ \mathrm{dB(A)}$) and the middle microphone becomes the loudest. This indicates, as expected, that the exhaust is not as dominant as for the full-load acceleration. The constant offset additionally indicates a generally better shielding of the front microphone, independent of position differences of individual sources like the inlet.

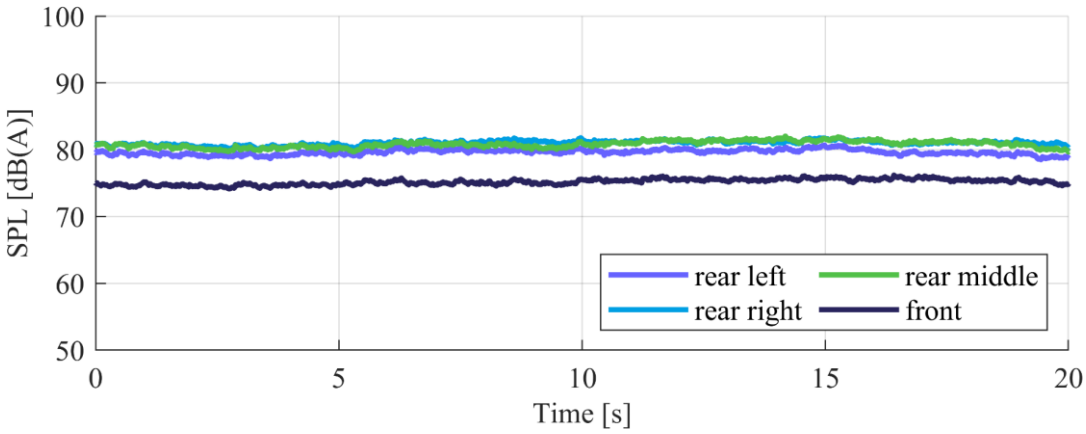

Figure 4-6: SPL vs. time for four microphone positions V1 constant speed 30 km/h

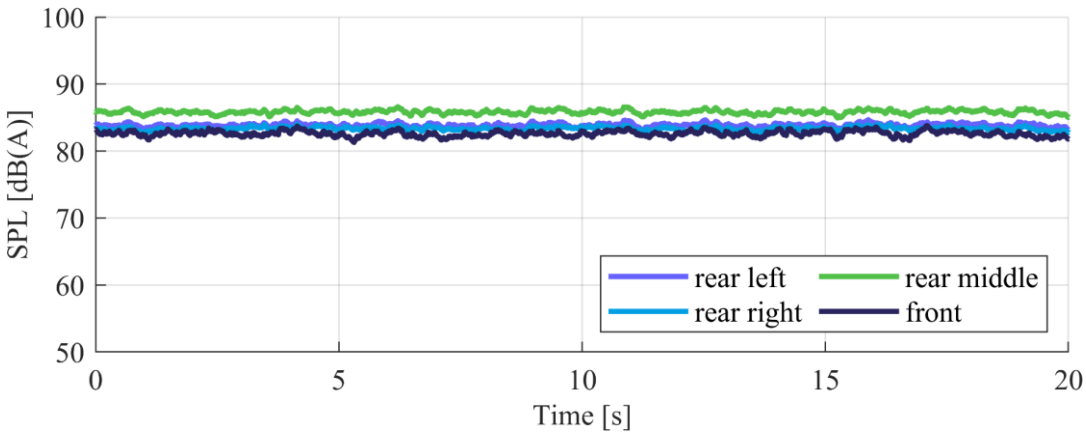

Figure 4-7: SPL vs. time for four microphone positions V2 constant speed 30 km/h

Although the A-weighting provides a good rough orientation with regard to the human perception of acoustic events, weaknesses often become apparent here, for example, when particularly loud events occur [13]. For this reason, the psychoacoustic quantity loudness shall be considered in a next step. This parameter is a sensation quantity and corresponds to human perception. A doubling of the value in [sone]

This project has received funding from the European Union's Horizon Europe research and innovation programme under grant agreement No 101056777

thus corresponds to a sound event perceived as twice as loud [14]. This is an advantage, especially with regard to the determination of relevant driving scenarios. For V1 the loudness is shown in Figure 4-8, for V2 in Figure 4-9. A similar behavior to the SPLs emerges, i.e., generally similar patterns for all microphones, and a significantly lower value for the front one. However, the mean standard deviation between the rear ones is 5.3 sone for V1 and 4.6 sone for V2. However, these standard deviations are not significant with respect to the absolute values of 100-150 sone. The previously mentioned effect becomes even clearer here, i.e., that the microphone on the right side tends to show higher values. The offset lies at 24.0 sone for V1 and 12.4 for V2. It is noticeable that the offset of the front microphone for V2 increases significantly in relative terms, which reinforces the importance of loudness consideration. Based on both the SPL and the loudness analysis, it can be concluded, that there are differences in the absolute values of the microphones, especially when the positions vary strongly, but there are no significant differences in the derivation of critical paths, i.e., no significant differences in the patterns. For this reason, and because of possible stronger asymmetries in future vehicles to be investigated, it is recommended to mount a microphone centrally in the rear area of the vehicle.

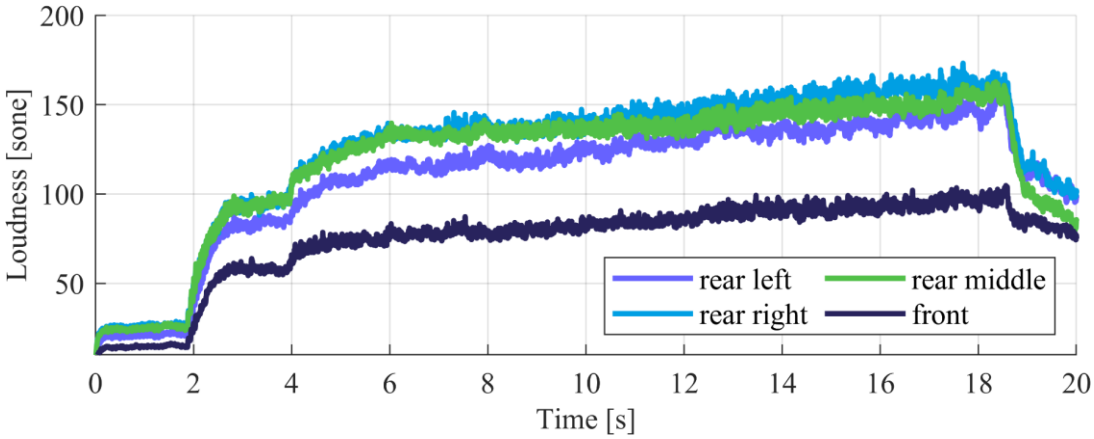

Figure 4-8: Loudness vs. time for four microphone positions V1 full-load acceleration

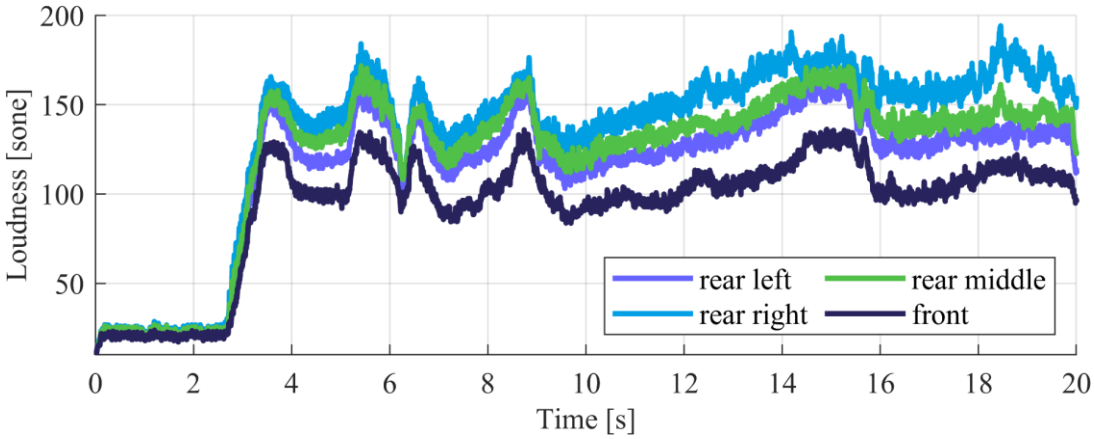

Figure 4-9: Loudness vs. time for four microphone positions V2 full-load acceleration

In a final step, the analysis will be extended to consider additional driving scenarios, both for SPL and loudness, for V1 and V2. The driving scenarios were recorded in separate measurement runs. For easier

This project has received funding from the European Union's Horizon Europe research and innovation programme under grant agreement No 101056777

comparability, all of them are presented in a continuous representation. SPL of V1 in Figure 4-10, SPL of V2 Figure 4-11, loudness of V1 in Figure 4-12 and loudness of V2 in Figure 4-13. The corresponding scenarios full load acceleration (FA), partial load (PA), constant driving (C), stationary partial (SP) and full (SF) rpm, coasting (CO) and test cycles (T) are marked in the figures. The test cycles T1 include FA to 30 km/h in the circle of the test track, three times straight FA to 50 km/h, coasting to 30 km/h. Test cycle T2 includes G3 FA to 30 km/h in the circle of the test track, straight FA to 50 km/h, comfort breaking to 10 km/h. The test cycles T3 include G2 FA to 30 km/h in the circle of the test track, four times straight FA to 50 km/h, coasting to 30 km/h. Furthermore, the background noise (BN) and idle have been recorded. For V2, different gears (G) are considered, i.e. second gear G2, third gear G3 and forth gear G4. The number in the diagram next to the condition abbreviations represent the vehicle speed in [km/h]. Due to the different types, performance and capabilities of the vehicles, the driven scenarios differ. All of the test scenarios reviewed confirm the results previously discussed by means of full-load acceleration. Only the offset of V2 varies between constant driving and acceleration scenarios between the three microphones in the back and the one in the front.

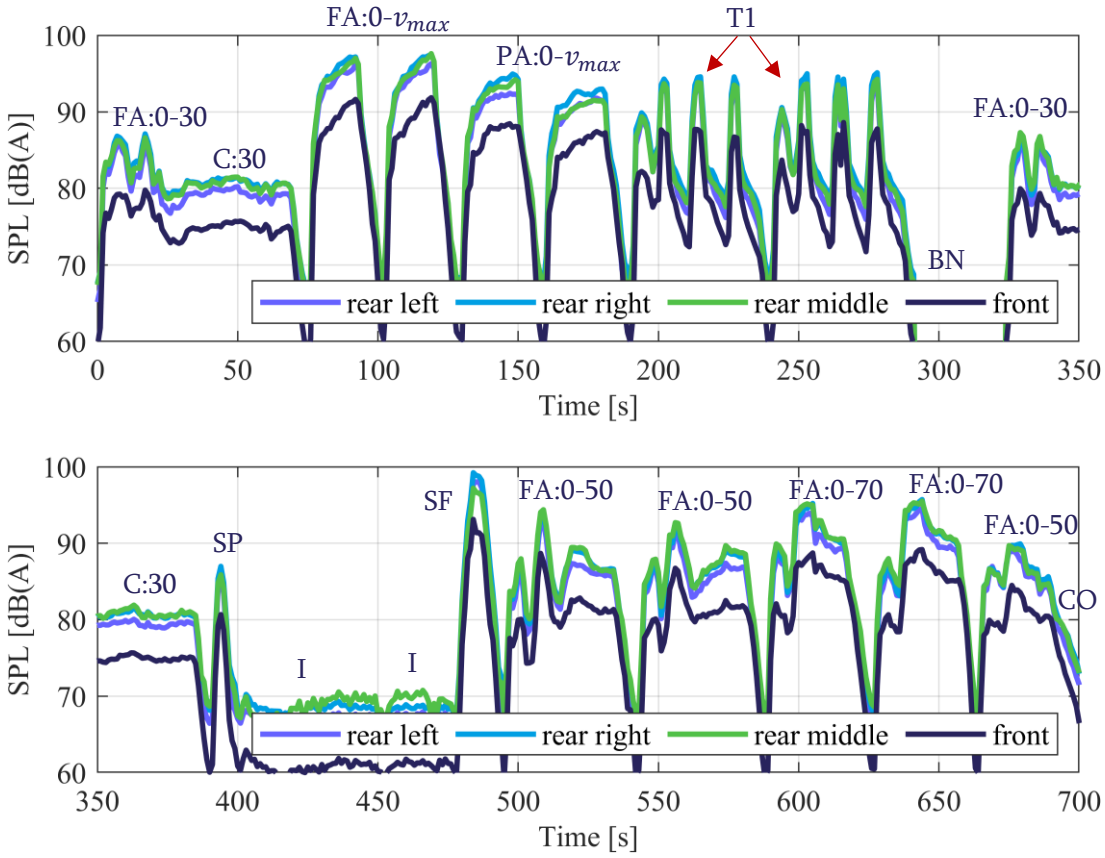

Figure 4-10: SPL vs. time for four microphone positions V1 for 33 different driving conditions

This project has received funding from the European Union's Horizon Europe research and innovation programme under grant agreement No 101056777

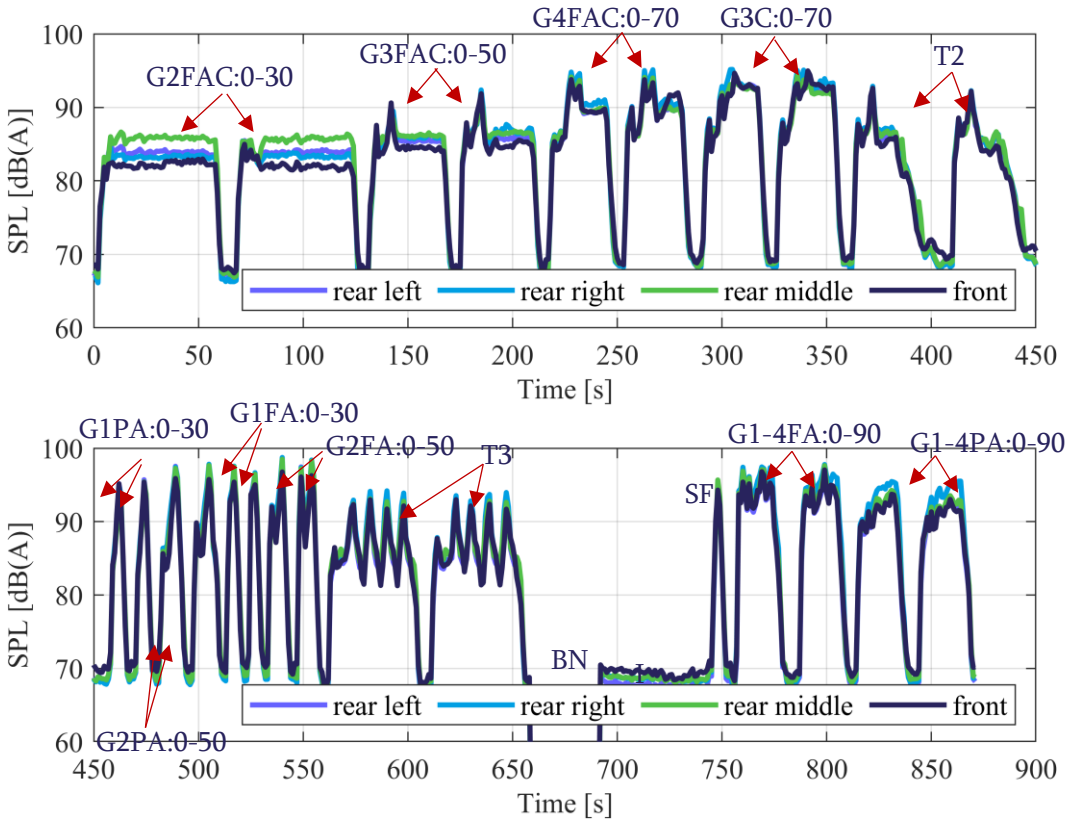

Figure 4-11: SPL vs. time for four microphone positions V2 for 39 different driving conditions

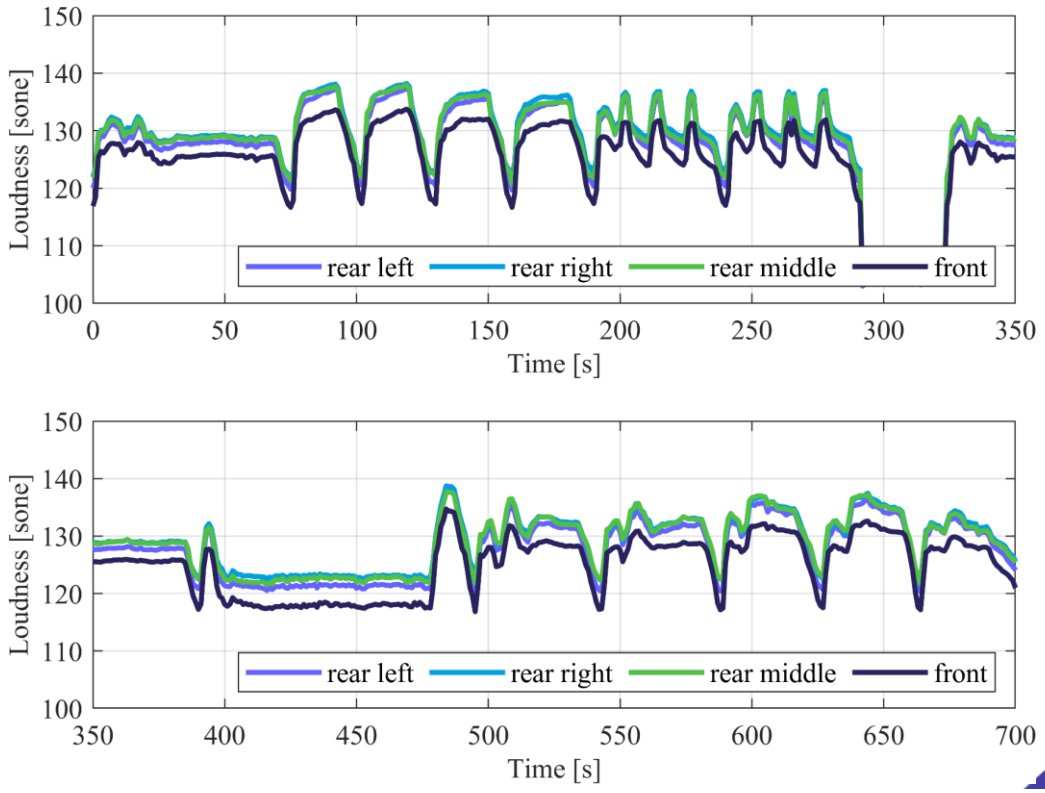

Figure 4-12: Loudness vs. time for four microphone positions V1 for 19 different driving conditions

This project has received funding from the European Union's Horizon Europe research and innovation programme under grant agreement No 101056777

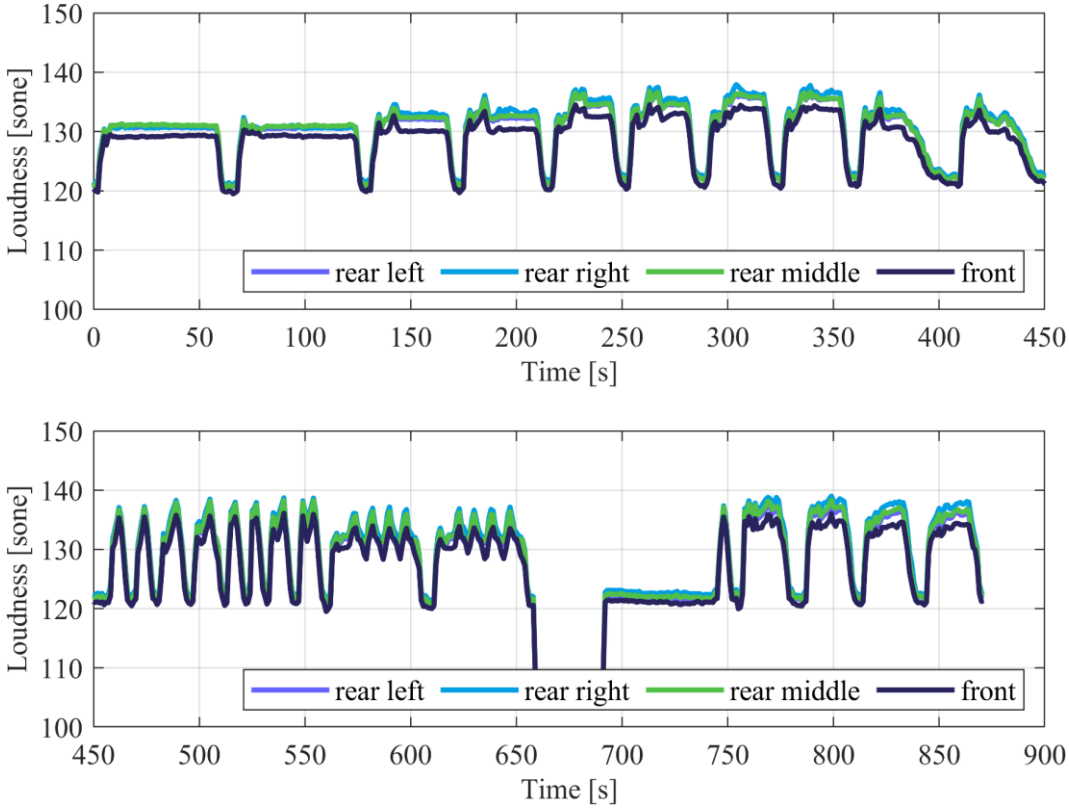

Figure 4-13: Loudness vs. time for four microphone positions V2 for 27 different driving conditions

This project has received funding from the European Union's Horizon Europe research and innovation programme under grant agreement No 101056777

5 Conclusion

L-category vehicles can cause high noise emissions. Therefore, the type approval tests for this vehicle category have been revised in the past. However, it is unclear, to which extent the actual type approval tests cover real-world driving patterns. The L-vehicles Emissions and Noise mitigation Solutions (LENS) project aims, among others, to develop techniques for monitoring noise emissions of L-category vehicles under real driving conditions. Hence, this deliverable describes the development process of an on-board sensor system for monitoring noise-critical driving scenarios.

In a first step, the components for the sensor system were selected. The system includes, among others, a microphone for monitoring noise emissions and a GPS module for tracking the position and speed of the vehicles. Both datasets are stored on a microSD card. In addition, to protect the components from environmental influences and to enable mounting on various vehicles, a mechanical housing was designed.

For the verification of the sensor system, a two-stage verification process in a semi-anechoic chamber was conducted. Various measurement setups were tested to determine the influence of additional components, the housing and the acoustic vent. The results showed that both affect the transmission behaviour of the sensor system. In addition, the sensor system was compared to a class 1 reference microphone. A major finding is that the sensor system is suitable for the monitoring of noise emissions.

In order to identify a suitable mounting position for the sensor system, measurements with four class 1 microphones on two exemplary vehicles were conducted. The key findings were, that the relevant frequency range is up to 3 kHz and frequencies above 5 kHz were negligible. Furthermore, the microphones positioned in the rear area show very similar patterns with marginal differences. Therefore, to conclude the position variation of the sensor system in the rear is negligible.

This project has received funding from the European Union's Horizon Europe research and innovation programme under grant agreement No 101056777

6 References

[1] Gunatilaka, Dolvara: An IoT-Enabled Acoustic Sensing Platform for Noise Pollution Monitoring. IEEE 12th Annual Ubiquitous Computing, Electronics & Mobile Communication Conference (UEMCON), 2021, pp. 0383-0389, doi: 10.1109/UEMCON53757.2021.9666534.

[2] Picaut, Judicaël et al.: Low-Cost Sensors for Urban Noise Monitoring Networks – A Literature Review. Sensors, 2020, 20(8):2256. https://doi.org/10.3390/s20082256.

[3] Peeters, Bert; v. Blokland, Gijsjan: The Noise Emission Model For European Road Traffic. IMAGINE project no. 503549, Deliverable 11, 2007, pp. 1-66.

[4] DFRobot: FireBeetle ESP32 IoT Microcontroller. Online: https://www.dfrobot.com/product-1590.html, access: October 07, 2023.

[5] Adafruit: Adafriut Ultimate GPS. Online: https://learn.adafruit.com/adafruit-ultimate-gps/overview, access: October 07, 2023.

[6] Adafruit: Adafruit I2S MEMS Microphone Breakout. Online: https://learn.adafruit.com/adafruit-i2s-mems-microphone-breakout, access: October 07, 2023.

[7] Knowles: SPH0645LM4H-B Rev B Datasheet I2S Output Digital Microphone. Online: https://cdn-reichelt.de/documents/datenblatt/A300/DEBO_MEMS_MIC_DB_EN.pdf, access: October 07, 2023.

[8] Adafruit: Micro SD Card Breakout Board. Online: https://learn.adafruit.com/adafruit-micro-sd-breakout-board-card-tutorial, access: October 07, 2023.

[9] FreeRTOS: Real-time operating system for microcontrollers. Online: https://www.freertos.org/index.html, access: October 07, 2023.

[10] GORE: Acoustic Vents. Online: https://www.gore.com/products/gore-acoustic-vents, access: October 07, 2023.

[11] STURM INDUSTRIES: STURM Nylon. Online: https://www.sturm.industries/sturm-nylon.html, access: October 07, 2023.

[12] ika test track: Application and Technical data. Online: https://www.ika.rwth-aachen.de/en/competences/equipment/infrastructure/ika-test-track.html, access: October 08, 2023.

[13] Fastl, Hugo: Gehörgerechte Geräuschbeurteilung. Lehrstuhl für Mensch-Maschine-Kommunikation, TU München, 1997, pp. 57-64.

[14] Zwicker, Eberhard: Psychoakustik. Springer, Berlin, Heidelberg, 1982.

[15] Kyulavska, Mariya; Toncheva-Moncheva, Natalia; Rydz, Joanna: Biobased Polyamide Ecomaterials and Their Susceptibility to Biodegradiation. Springer, Cham, 2017, pp. 1-34, https://doi.org/10.1007/978-3-319-48281-1_126-1.

[16] Diemel, Carina; Uszynski, Olaf; Yordanov, Ventseslav; Städtler, Leonhard: Sensor System for Noise and Positioning Data Acquisition. ATZ worldwide, 2023, No. 11, pp. 30-35.

This project has received funding from the European Union's Horizon Europe research and innovation programme under grant agreement No 101056777

Funded by the European Union. Views and opinions expressed are however those of the author(s) only and do not necessarily reflect those of the European Commission or CINEA. Neither the European Commission nor CINEA can be held responsible for them.